ISBN: 978-3-95450-247-9 ISSN: 2673-5490 doi: 10.18429/JACoW-IPAC2024-MOPS59

FAST-RAMPING ALPHA MAGNET FOR INTERLEAVED OPERATION AT ANL APS*

Y. Chen†, R. Agustsson, T. Hodgetts, C. Oberempt, Radiabeam, Santa Monica, CA, USA
G. Waldschmidt, W. Berg, D. Bianculli, A. Jain, M. Jaski, K. Wootton,
Argonne National Laboratory, Lemont, IL, USA

Abstract

RadiaBeam is designing and manufacturing a fast-ramping alpha magnet developed for interleaved operation at the Argonne Advanced Photon Source (APS). This interleaving operation requires the alpha magnet to stably complete a 5 s long cycle with a 100 ms ramp-up, 1000 ms nominal field output and a 100 ms ramp-down. A laminated yoke is used to minimize eddy currents, ensure fast field response time, and reduce core-loss during operation. The magnetic and mechanical design demonstrating the performance of a 2.75 T/m maximum field gradient alpha magnet within a 10 cm x 14 cm good field region will be presented along with the current fabrication status.

INTRODUCTION

The interleaved operation at the Argonne National Laboratory (ANL) Advanced Photon Source (APS) linac shown in Figure 1 requires fast switching between two injections occurring every cycle [1-3]:

- RG2 RF thermionic electron gun into Particle Accumulator Ring (PAR).
- RF photocathode electron gun (PCG) into Linac Extension Area (LEA) [4].

This cannot be achieved with the existing alpha magnet, whose switching frequency is limited by its solid core. The replacement fast-ramping alpha magnet therefore needs to operate with 5 s period and 100 ms rise/fall time. The pulse length for the RG2 RF gun injection is 1 s with an additional 100 ms rise and fall time During the 3.8 s downtime for PCG operation, the magnet operates with a small reverse current to offset the remnant field so the PCG can inject without deflection of the beam. The power supply needs to be both programmable and bipolar.

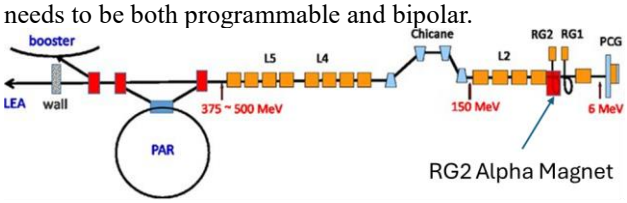

Figure 1: Layout of APS linear accelerator. The fast-ramping alpha magnet is designed to replace the existing RG2 Alpha Magnet.

In addition, the alpha magnet also operates in DC mode at the nominal current to for setup and diagnostic testing of the electron beam from the RG2 RF gun. A degaussing process is necessary to remove any magnetic field during diagnostic testing. The heat generation in DC mode requires the coil to be constantly water-cooled.

The magnet core is laminated to minimize the in-core eddy current and the transient effect on the generated magnetic field. Further, simulation shown in later sections demonstrate that we cannot ignore the eddy currents in the stainless-steel chamber during ramping.

The critical parameters of the alpha magnet were specified by ANL and shown in Figure 2 and Table 1.

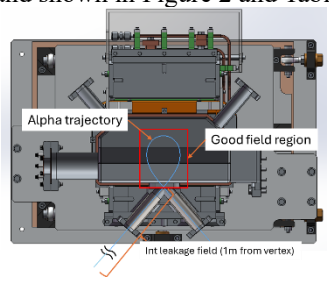

Figure 2: Illustration of Alpha trajectory and path for defining the integrated leakage field of the alpha magnet.

Table 1: Field Parameters of Fast Ramping Alpha Magnet

Parameters	Requirement	Unit
Field gradient	2.75/2.46	T/m
Beam energy	2.0/3.0	MeV
Bend angle	278.6	Deg
Input/output angle	81.4	Deg
Vertical aperture	≥24	mm
Good field region	10 x 14	cm
Field variation in GFR	±1.5%	-
Int. leakage field (1m)	≤0.5	G·cm

MAGNETIC DESIGN

Static Field Simulation

The magnetic design of alpha magnet starts with the 2D hyperbolic pole face function [5]:

$$y\,(x) = \frac{h}{1+B'x/B_0} \qquad (1)$$

The parameters are:

- h = 75 mm is the vertical height at origin.
- B′ = 2.75 T/m is the designed gradient.
- B_0 = 0.10 T is the magnetic field at origin.

The pole face is defined as starting at the origin and truncates at x=130 mm, as shown in Figure 3. The parameters and ranges are chosen to generate a field profile that satisfies the field variance requirement within the Good Field

* Work supported by the U.S. Department of Energy, Office of Science, Office of Basic Energy Sciences, under Contract No. DE-AC02-06CH11357 and DE-SC0015191.
† ycchen@radiabeam.com

ISBN: 978-3-95450-247-9 ISSN: 2673-5490 doi: 10.18429/JACoW-IPAC2024-MOPS59

Region (GFR) and vertical aperture. B' and B_0, determine the x position of the vertical asymptote of the hyperbola. The magnetic field is zero at that location and will increases linearly with a slope of B'. The intersection of the vertical asymptote and the x axis defines the ideal vertex of the alpha trajectory. For optimal performance, the inner edge of the beam-side return yoke (a.k.a., the mirror plate) is coplanar with the asymptote to confine the returning magnetic flux so leakage field at vertex can be minimized.

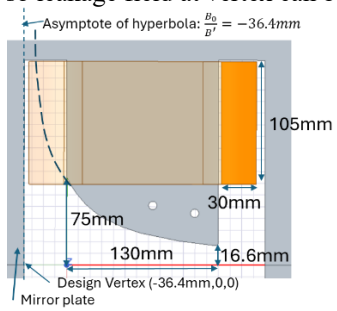

Figure 3: The design of pole face, return yoke, and coil cross-section of alpha magnet.

An aperture for the beam near the vertex leads to field leakage and distorts the ideal field profile. This Y-shape aperture is created on the mirror plate to accommodate the inlet and outlet beampipes on the chamber while minimizing the undesirable field perturbations. Figure 4 shows the field in the alpha magnet vs x axis. The field starts increasing before the vertex and reaches 120 G at the vertex. The field gradient gradually increases with field and reaches 2.75 T/m at x=-18 mm. The field variance is 13.8% in the range x= [-36.4 mm, -18 mm] and is within 1.5%, per the specification, in the range x= [-18 mm, 110 mm]. Figure 5 shows the field variance in GFR on y=0 plane through the center of the magnet. The presence of magnetic field at the input of the magnet introduces extra bending to the beam before and after the alpha loop. The total integrated leakage field along a 1m path leading to the vertex is 4.02 G·cm.

To validate baseline performance, single particle tracking was performed using the 2D field map from the ANSYS-MAXWELL magnetic field simulations. The results are presented in Figure 6. The alpha trajectory intersects near the ideal vertex position with ~2 mm offset. Further, ANL performed beam physics analysis with a complete 3D field map and approved the static field performance of the design.

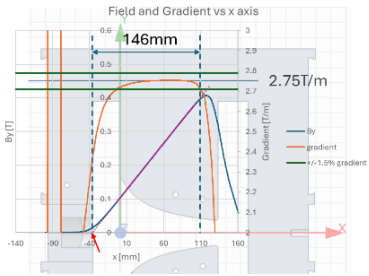

Figure 4: Field and gradient profile at 2.75 T/m output. The window on the mirror plate results in non-zero field and gradually increasing gradient around the vertex, illustrated by the red arrow.

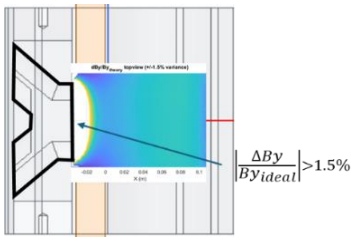

Figure 5: 2D field variance plot inside GFR on y=0 plane. Field variance exceeds 1.5% in the white area near the window but is under 1.5% elsewhere.

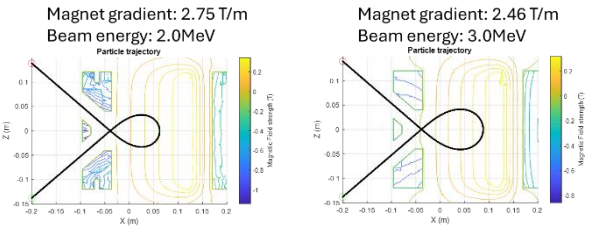

Figure 6: Single particle tracking results of 2 MeV beam in a 2.75 T/m gradient (left) and 3 MeV beam in a 2.46 T/m gradient (right).

Transient Simulation

The main focus of the transient study is to assess the magnetic field response to a single cycle of the pulsed current input. The transient model includes a simplified vacuum chamber, end plates, coil support, chamber support, and fasteners near the GFR. Figure 7 shows the gradient output during 100 ms ramping and 1 s pulse time. The gradient is 98.9% of nominal after ramping up. The output reaches 99.98% nominal gradient 200 ms later and outputs 100% nominal gradient for the remaining 800 ms pulse time. This result is confirmed by observing the cessation of eddy currents in the chamber.

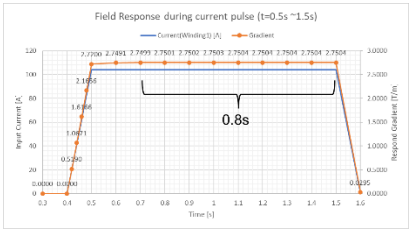

Figure 7: Gradient output during ramping and pulse.

The simulation evaluated heat generation from the coil, magnet yoke, chamber and the hardware. Heat generation from eddy current loss and hysteresis loss were determined to be negligible. The average heat generation in pulse mode was 163 W from the ohmic loss in the coil. For comparison, the power consumption in DC mode was 772 W. With proper cooling, the temperature rise in either mode should not exceed 5 °C.

Another transient effect is the vibration due to periodic magnetic forces. The chamber, with its noticeable eddy currents, experiences alternating forces during ramping cycles. The force is less than 8 N and can be handled by fasteners. The forces on the yoke and coil are in phase with pulsing and does not exceed the limit of the supporting and fastening mechanisms in either operating mode.

ISBN: 978-3-95450-247-9 ISSN: 2673-5490 doi: 10.18429/JACoW-IPAC2024-MOPS59

The strength of the remnant field is not simulated in this study and will be determined in field measurement. The power supply is bipolar and will output reversed current to offset the remnant field. A power supply and controller with approximately 50 ppm ripple and 100 ppm stability or better is specified to accomplish this task.

The peak current and voltage for 2.75 T/m gradient output in pulse mode is 104 A and 32.5 V. A pair of IECO BPS-85-70 bipolar power supplies, wired in parallel, [6] were selected to output a total of 140 amps at 85 volts. A control system, to be developed by ANL, will generate the source signal and monitor the actual output current.

MECHANICAL DESIGN

Yoke

The alpha magnet is a two-piece assembly split at the horizontal mirror plane. Each yoke-half is made from Cliffs/AK Steel DI-MAX M-19 steel lamination with .625mm thickness. The laminations are bonded with epoxy and cured at high pressure. To further secure the bonding, the yoke-half is sandwiched by two 9.53-mm-thick stainless steel end plates. Machining on the yoke-halves is minimized due to the precision laser cutting and stacking tooling. The magnet halves are match-drilled as an assembly to ensure precision alignment and repeatable construction.

The top and bottom yoke-halves are held together with two clamps. The clamp at the beam entrance side has windows for the input and output beampipes. The same clamp-on extrusions on the top and bottom corners are used in lifting and stage-clamping.

There is a 170.2 mm x 76.2 mm window on the yoke for beam entrance. The window is not machined but comes from different steel lamination with shorter leg geometries. A pair of insertion pieces will be used to fill the gap, as much as possible, at the window with Y-shape tunnel cut out carefully machined into the laminated steel block to reduce leakage magnetic field. The outer dimension will be machined to the size of the rectangular window on the yoke-half. The x position of insertion piece is secured with pins. The fully engineered model is presented in Figure 8.

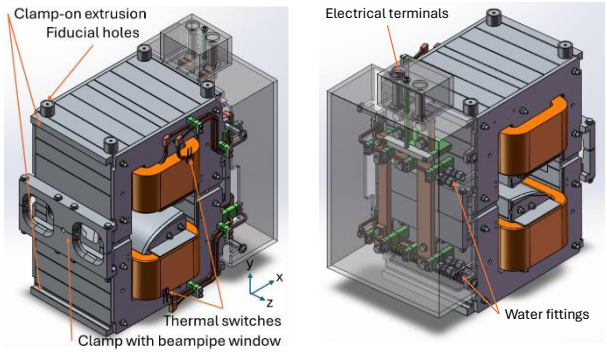

Figure 8: Angle view from beam entrance side (left). Angle view from the terminal side (right).

Coil

The coil has 58 turns. The conductor size is 6.35 mm square with Ø3 mm ID for direct water cooling. In DC mode, the power consumption is 772 W. When coil is directly cooled by 50 psi, 0.68 GPM water flow, the estimated temperature rise is 4.1 °C. Thermal switches and thermocouples are installed on the coil and magnet pole for safety monitoring.

The coil is vacuum encapsulated in epoxy to prevent damage. When curing in vacuum, epoxy fills the gap between conductors. Epoxy improves inter-conductor insulation and prevents vibrational wearing inside coil when operating in pulsed mode. The epoxied coil is firmly assembled to the yoke-half with support brackets and G-10 pads are inserted at all contact surfaces on the coil. The electrical terminals, water fittings, and thermal sensor terminals are located on the opposite side of the beam entrance, covered by a transparent polycarbonate box. To sum up, the design parameters are presented in Table 2.

Table 2: Parameters of the Fast-Ramping Alpha Magnet

Parameters	Design	Unit
Footprint (L x W x H)	503x349x572	mm
Field gradient	2.75	T/m
Magnet aperture	33	mm
Good field region	10 x 14	mm
Field variation		-
-36.4 mm<x<-18 mm	13.7%	-
-18 mm<x<110 mm	<1.5%	-
Int. leakage field	4.02	G·cm
Operating current	104.1	A
Voltage (peak)	32.5	V
Resistance	71	mΩ
Inductance	24.2	mH
Pulse mode period	5	s
Ramp time	0.1	s
Current density	4.9	A/mm^2
Power (DC)	772	W
Temperature rise (DC)	4.1	°C
Cooling H20 pressure	50	psi
Net water flow	0.68	GPM
Weight	703	lb

CURRENT FABRICATION STATUS

We have completed the coil winding process. The epoxy mold has been assembled and tested. Following an epoxy process validation with a dummy coil, the actual coils will be impregnated. The steel laminations of two geometries have been received and inspected by sampling. The fixture for lamination stacking and pressing are undergoing evaluations. Radiabeam received the bipolar power supplies from the vendor and performed preliminary testing on both units. Remote control and low current output were verified prior to delivery to ANL for further validation.

ACKNOWLEDGEMENTS

Work supported by the U.S. Department of Energy, Office of Science, Office of Basic Energy Sciences, under Contract No. DE-AC02-06CH11357 and DE-SC0015191.

ISBN: 978-3-95450-247-9 ISSN: 2673-5490 doi: 10.18429/JACoW-IPAC2024-MOPS59

REFERENCES

[1] Y. Sun *et al.*, "APS LINAC Interleaving Operation", in *Proc. IPAC'19*, Melbourne, Australia, May 2019, pp. 1161-1163. doi:10.18429/JACoW-IPAC2019-MOPTS119

[2] S. Shin, Y. Sun, J. Dooling, M. Borland and A. Zholents, "Interleaving lattice for the Argonne Advanced Photon Source linac," *Phys. Rev. Accel. Beams*, vol. 21, p. 060101, Jun. 2018. doi:10.1103/PhysRevAccelBeams.21.060101

[3] J. Lewellen, private communication, Feb. 2001.

[4] W. Berg, J. C. Dooling, S. H. Lee, Y. Sun, and A. Zholents, "Development of the Linac Extension Area 450-MeV Electron Test Beam Line at the Advanced Photon Source", in *Proc. IBIC'19*, Malmö, Sweden, Sep. 2019, pp. 219-221. doi:10.18429/JACoW-IBIC2019-MOPP048

[5] J. T. Tanabe, "Iron Dominated Electromagnets: Design, Fabrication, Assembly and Measurements," Singapore: World Scientific Publishing Co., 2005. doi:10.1142/5823

[6] *Bipolar Power Supply*, Oy International Electric Co., Helsinki, Finland, 2020; https://www.ieco.fi/doc/BPS-85-70_revB_EMEA.pdf